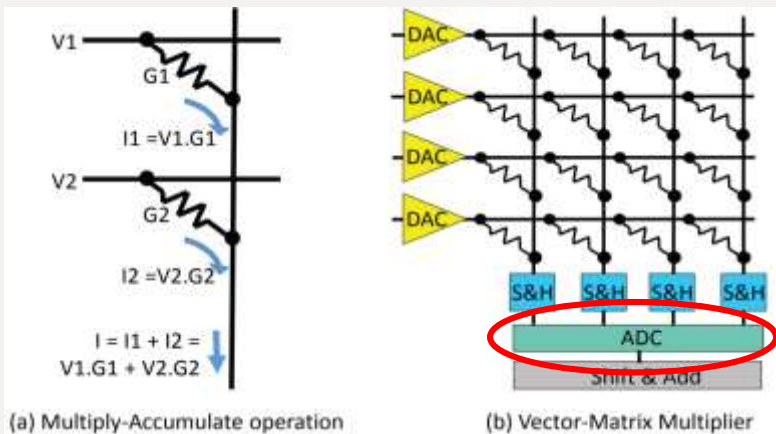
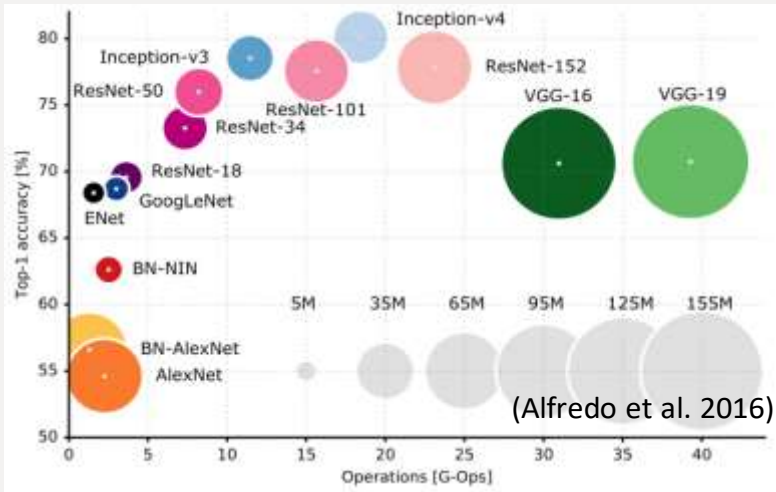


Exploring Bit-Slice Sparsity in Deep Neural Networks for Efficient ReRAM-Based Deployment

Jingyang Zhang¹, **Huanrui Yang**¹, Fan Chen¹, Yitu Wang², Hai Li¹

¹Duke University, ²Fudan University

Motivation: ReRAM-based DNN accelerator



- High bit-resolution ADC accounts for >60% power and >30% area
- ADC resolution dictated by accumulated currents on bitlines: need sparsity in G
- Limited cell bit density: each XB only holds 2 bits (bit-slice) of the weight
- Need **higher sparsity among bit-slice**

$$\begin{bmatrix} 0 & w_1 & 0 \\ 0 & 0 & w_2 \\ w_0 & 0 & 0 \end{bmatrix} \Rightarrow [11\ 00\ 10\ 00]_2$$

Weight sparsity Bit-slice sparsity

Two-order magnitude advantage in energy, performance and chip footprint

Canziani, Alfredo, Adam Paszke, and Eugenio Culurciello. "An analysis of deep neural network models for practical applications." *arXiv preprint arXiv:1605.07678* (2016).

A. Shafiee, A. Nag, N. Muralimanohar, R. Balasubramonian, J. P. Strachan, M. Hu, R. S. Williams, and V. Srikumar. Isaac: A convolutional neural network accelerator with in-situ analog arithmetic in crossbars. In Proceedings of ISCA, 2016.

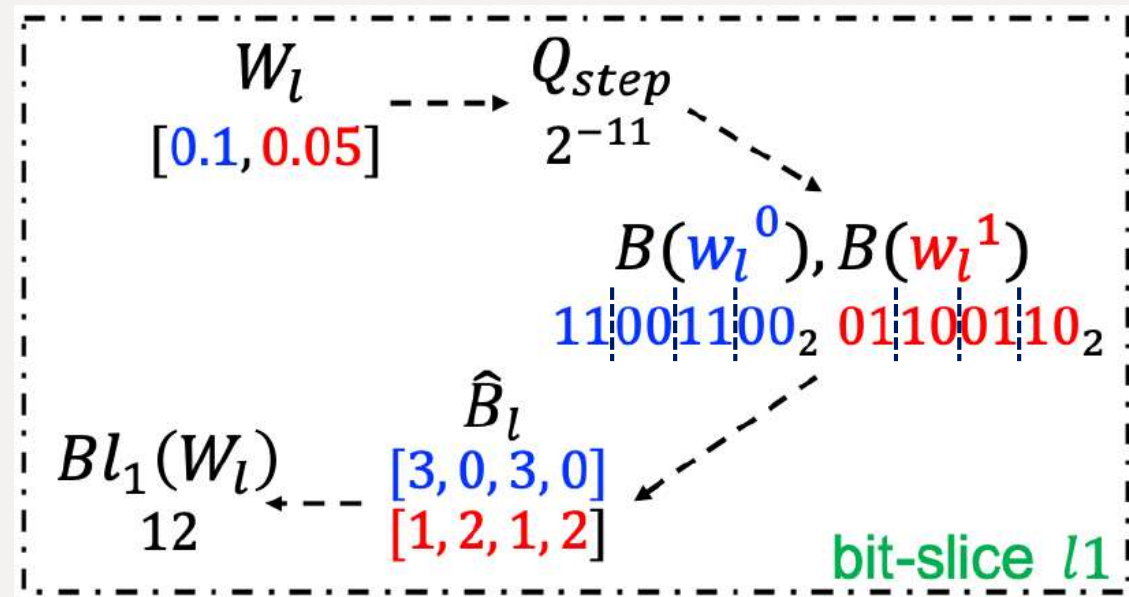
Bit-slice L1 for dynamic fixed-point quantization

- Dynamic range scaling (to [0,1])

$$S(W_l) = \lceil \log_2(\max_{w_l^i \in W_l} (|w_l^i|)) \rceil,$$

- N-bit uniform quantization

$$Q_{step} = 2^{S(W_l) - n}, \quad B(w_l^i) = \lfloor \frac{w_l^i}{Q_{step}} \rfloor.$$



- L1 regularization over all bit-slices

$$B(w_l^i) = \sum_{k=0}^3 \hat{B}_l^{i,k} \cdot 2^{2k} \quad Bl_1(W_l) := \sum_{i,k} \hat{B}_l^{i,k}.$$

Training routine

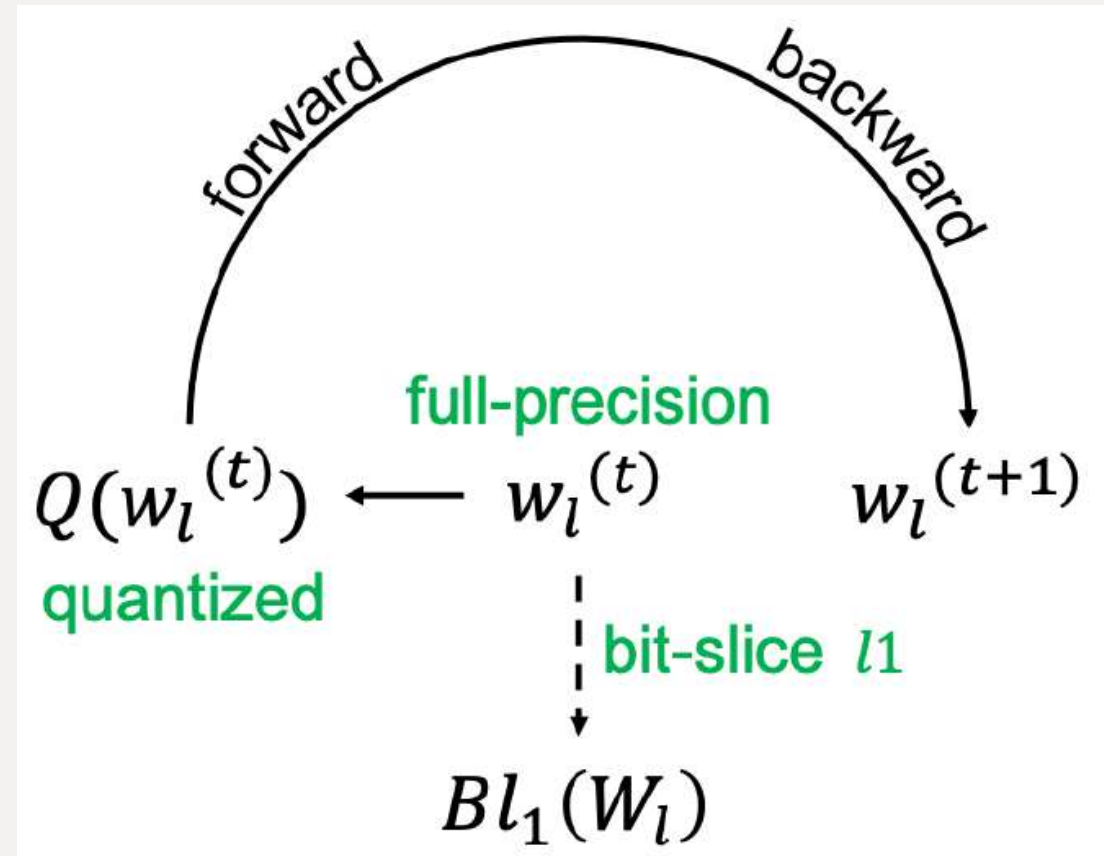
- Dynamic range recovery

$$Q(w_l^i) = B(w_l^i) \cdot Q_{step}$$

- Training routine
 - FP and BP with quantized weight
 - Gradient update on full-precision weight
 - Add Bit-slice L1 to the objective

$$q^{(t)} = Q(w_l^{(t)}),$$

$$w_l^{(t+1)} = q^{(t)} - lr \times (\nabla_q \mathcal{L}_{CE}(q^{(t)}) + \alpha \nabla_q Bl_1(q^{(t)}))$$



Improving the bit-slice sparsity

- Up to 2x less nonzero bit-slices than traditional L1

Table 1: Results on MNIST

Method	Accuracy	Ratio of non-zero wights				Average
		\hat{B}^3	\hat{B}^2	\hat{B}^1	\hat{B}^0	
Pruned	97.99%	1.08%	5.87%	8.42%	17.42%	8.20±5.94%
ℓ_1	97.99%	1.19%	5.21%	7.01%	11.36%	6.19±3.65%
$B\ell_1$	97.67%	0.84%	4.02%	4.27%	9.58%	4.68±3.14%

Table 2: Results on CIFAR-10

Model	Method	Accuracy	Ratio of non-zero wights				Average
			\hat{B}^3	\hat{B}^2	\hat{B}^1	\hat{B}^0	
VGG-11	Pruned	88.93%	0.86%	28.30%	34.14%	33.39%	24.17±13.65%
	ℓ_1	89.39%	0.39%	9.37%	18.43%	22.19%	12.59±8.45%
	$B\ell_1$	89.33%	0.21%	3.57%	7.09%	10.71%	5.40±3.92%
ResNet-20	Pruned	89.22%	1.10%	8.07%	21.92%	43.96%	18.76±16.36%
	ℓ_1	90.62%	0.44%	4.71%	14.37%	33.16%	13.17±12.60%
	$B\ell_1$	89.66%	0.31%	3.34%	11.99%	31.39%	11.76±12.12%

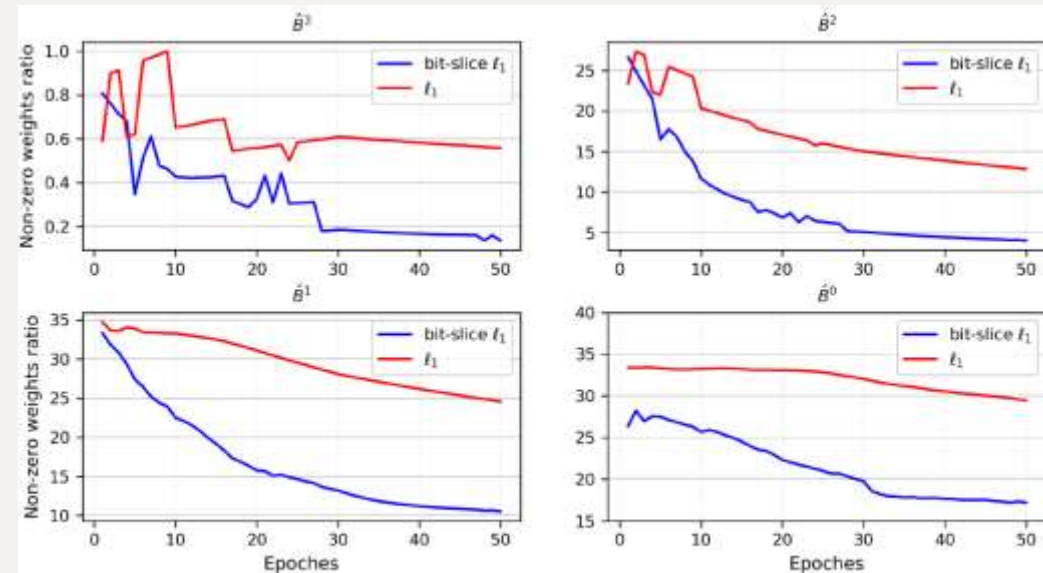


Figure 2: Bit-slice sparsity of VGG-11 on CIFAR-10 during training.

- Codes available at: https://github.com/zjysteven/bitslice_sparsity Duke

Reducing ADC overhead

- High sparsity in bit-slices enables the use of low-resolution ADC
- Low resolution reduces ADC overhead
- Simulation results for mapping to 128x128 ReRAM XBs

Table 3: ADC Overhead Saving with Bit-Slice Sparsity

	w/o Bit-Slice Sparsity		w/ Bit-Slice Sparsity		
	Resolution	Resolution	Energy Saving	Speedup	Area Saving
XB_3	8 bit	1 bit	28.4×	8×	2×
$\text{XB}_{2,1,0}$	8 bit	3 bit	14.2×	2.67×	2×